Passive Compliant Mechanism Based Knee Exoskeleton to Alleviate Knee Joint Moment of Workers During Blueberry Harvesting

Leanne Hofer-Nigg*, Ben McGuinness, Christoff Venter, Eva Prinz, Hung Phan Le, Mike Duke and Ajit Pal Singh**
School of Engineering, University of Waikato, New Zealand
lh232@students.waikato.ac.nz*, ajitpal.singh@waikato.ac.nz**

Abstract

The blueberry industry is a key contributor to the New Zealand economy but is currently facing labour shortages that threaten yield security. Blueberry harvesting is physically demanding, limiting the available workforce. Fully autonomous solutions are financially unfeasible and compromise the berry marketability. As an intermediate solution, this paper develops a passive robotic knee exoskeleton designed to reduce the knee moment experienced by workers while harvesting. The device utilises compliant mechanisms to store elastic energy and assist users in rising from a deep squat. Presented in this paper is the optimisation of a linear compliant mechanism to deliver 117.85 N, based on the knee moment of a 43.46 kg human during squatting. FEA was used to optimise the mechanism shape and dimensions to achieve a uniform stress distribution across the material. Simulation with nylon-6-PLA achieved 100% of the target force with a stress safety factor of 1.56. A CNC-machined prototype was compression tested, revealing that 67% of the knee moment could be alleviated. Despite the deviation from FEA, results suggest compliant mechanisms can be effectively integrated into a passive knee exoskeleton to reduce the knee moment of blueberry harvesters.

1 Introduction

Over recent years, blueberries have gained popularity globally, becoming the second most prominent soft fruit due to increased consumption [1]. Being labelled as a “super fruit” due to the health benefits associated with blueberry consumption has contributed to this surge in popularity. This is highly beneficial to New Zealand as the horticulture industry plays a vital role in the economy, contributing over $7.5 billion for the year of 2024/25 [2]. Within this sector, there has been an obvious increase in blueberry production to meet the rising demands, with 4000 tonnes of blueberries produced in New Zealand in 2023/24 [3].

Although this rising demand shows strong potential for the New Zealand economy, the blueberry industry faces some challenges that cannot be overlooked. Blueberry harvesting is an incredibly physically demanding job that subjects workers to immense stress on their body over prolonged periods of time [4]. While harvesting, workers are required to tolerate uncomfortable postures (Figure 1) and undertake physically demanding repetitive tasks for extended periods to reach fruit on all heights of the shrubs.

Figure 1: Postures for hand harvesting of blueberries.

These postures can lead to immense fatigue in workers, resulting in decreased efficiency and can pose risks to their health. Common for workers in the agriculture industry, physical demands can lead to an increased risk of injury such as developing musculoskeletal disorders [5]. As a consequence, there is a reduced demographic capable to undertake the work, leading to labour shortages in the New Zealand blueberry industry [6]. Such labour shortages can be detrimental to the industry as an insufficient workforce means harvesting may not be completed quickly enough, causing blueberries to over-ripen, increasing disease susceptibility, dehydration and shortening shelf time [7].

To address such challenges, fully autonomous solutions have been explored in industry, such as machine harvesting. This poses significant challenges, not only due to high costs making this unfeasible for many orchard owners but also due to the increased risk of damaging the soft fruit. Blueberries are highly delicate and perishable which causes them to be easily damaged during harvesting. A major risk with utilising fully automated machinery for harvesting is reducing the quality of the berries, limiting the shelf life and marketability [8].

Alternatively, these issues can be mitigated by implementing an intermediate solution of robotic wearable devices, such as exoskeletons. Exoskeletons are wearable mechanisms, designed to physically assist users by mimicking the biomechanics of the human body [9]. These robotic devices can be either active or passive, where an active design utilises an external energy source to power the exoskeleton. This project aims to alleviate the issues involved in blueberry harvesting, by designing a novel passive knee exoskeleton, the Compli-Knee, that reduces the knee joint moment in users during harvesting.

This paper investigates the use of compliant mechanisms for integration into exoskeletons for blueberry harvesting. Compliant mechanisms utilise elastic deformation of a material to achieve a desired outcome [10]. Implementing compliant mechanisms in the Compli-Knee will utilise negative work from the user to convert gravitational energy to elastic energy during squatting. The force output will assist the user to stand up, hence reducing the knee joint moment experienced. Introducing such mechanisms in this application is highly beneficial due to their low cost, lightweight and environmentally sustainable features.

Key exoskeleton design considerations are to ensure devices are lightweight and have minimal impedance on the body. Many studies investigating exoskeleton design highlight the importance of minimising impedance [11], [12], [13], [14]. Moreover, any misalignment between the exoskeleton and human joint can lead to injury, which can be mitigated with the use of compliant mechanisms [11]. There is currently very limited research on both exoskeletons for the agriculture industry as well as the utilisation of compliant mechanisms in exoskeletons.

The Compli-Knee is a development to bridge the gap between physical manual labour and fully autonomous solutions. With the current unfeasible nature of autonomous machinery for blueberry harvesting, the robotic human assistive exoskeleton will ensure high yield quality is met which can currently only be achieved with harvesting by hand. Additionally, the Compli-Knee will make physically demanding tasks more achievable, hence increasing the demographic that is able to undertake the work and potentially improve the appeal of blueberry harvesting as a job.

2 Experimental Procedure

2.1 Design Requirements

The most important design specification was the force output required of the compliant mechanism, based on the knee joint moment during blueberry harvesting. [15] and [4] evaluated different postures and ergonomics of workers during hand blueberry harvesting. Deep squatting was found to be a common technique used to reach the low hanging fruit. Consequently, the knee joint moment and Range Of Motion (ROM) for deep flexion was evaluated.

The knee flexes to 160° from standing to a deep squat, corresponding to a final knee flexion angle of 20° [16]. The knee joint reaches a maximum moment (M) of 0.93 ± 0.16 Nm/kg when lowering to a squat/rising from deep kneeling [17]. [18] found that the knee moment increases during a squat, reaching a maximum moment at ~150° before reducing slightly when deep flexion is reached. As a result, a constant knee moment is assumed for the design of the Compli-Knee.

The location of the force acting on the leg was aligned with the thigh centre of mass to minimise additional metabolic cost from the exoskeleton [19]. The distance from the knee joint to mechanism contact point of the thigh, T and shank, S are calculated from Equations 1 and 2.

$$T = U \cdot 0.567 \qquad (1)$$

where U is the total upper leg length

$$S = \frac{T}{\cos\theta_f} \qquad (2)$$

where θ_f is the final knee flexion angle

The anthropometric values were finalised based on a range of results from literature [20], [21], [22], [23], [24]. The average values for females and males were used.

θ_i was set based on the point of thigh to calf contact during squatting (45.2°). This angle was chosen as the tissue contact significantly reduces the knee joint forces in a deep squat [17], [25].

The distance between the thigh and calf contact points (C) for initial (i) and final (f) conditions can be calculated using Equations 3 and 4.

$$C_i = \sqrt{T^2 + S^2 - 2 \cdot T \cdot S \cdot \cos(\theta_i)} \qquad (3)$$

$$C_f = T \cdot \tan\theta_f \qquad (4)$$

The total displacement (D) of the linear compliant mechanism is

$$D = C_i - C_f \qquad (5)$$

Holding C_f constant, D was increased from 106.1 mm to 112 mm to maximise the displacement. Hence, θ_i was increased to 46.65° based on

$$\theta_i = cos^{-1}(\frac{T^2 + S^2 - D^2}{2 \cdot T \cdot S}) \tag{6}$$

The force requirement was designed for a 43.46 kg person based on a 95% confidence for the female population [20]. The lower percentile was selected, as designing for heavier individuals would limit the ability of lighter users to fully compress the mechanism. The total force requirement of 117.85 N was calculated using

$$M = F \cdot T \tag{7}$$

Figure 2 shows the design criteria, assuming the knee is pin jointed.

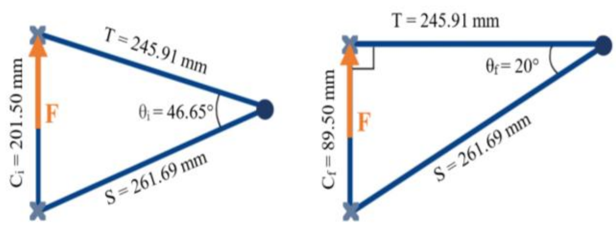

Figure 2: Design criteria for the Compli-Knee, initial state, i (left) and final state, f (right).

2.2 Compliant Mechanism Optimisation Using FEA

Finite Element Analysis (FEA) was used to determine whether a linear compliant mechanism can supply a sufficient force for use in a knee exoskeleton. Optimisation was performed to achieve a Stress Safety Factor (SSF) of at least 1.5. SolidWorks FEA was used to simulate the mechanism performance with prescribed displacements.

Initially, a comparison between two linear nodes, the X-Bob and LET (Lamina Emergent Torsional), was undertaken. The shape of a single unit of each mechanism can be seen in Figure 3, with the key dimensions labelled. Original dimensions for each mechanism can be found in Table 1, where z indicates the thickness of the mechanism.

A prescribed displacement of 21.2 mm was applied to each mechanism unit separately, based on 5 units for a total displacement of 106.1mm. SLS printed nylon material properties were used, obtained from Type 3 dog-bone samples as per the ASTM D638 standard. The stiffness and yield strength values were 1640 MPa and 37.79 MPa, respectively.

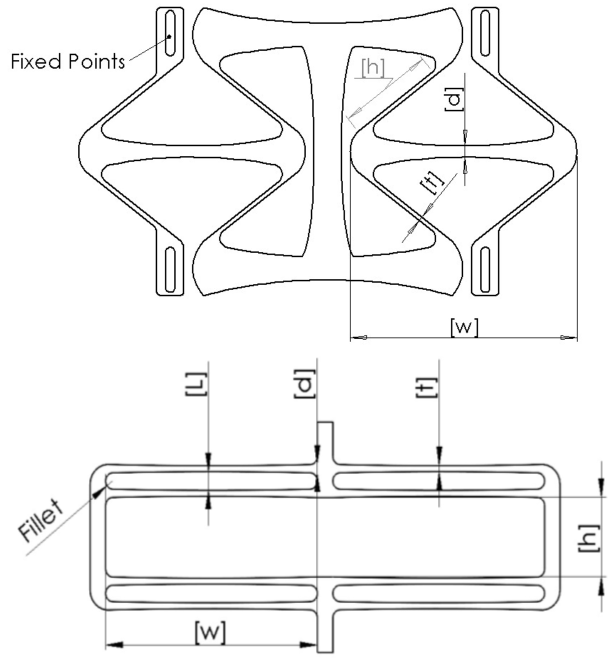

Figure 3: Shape and key dimensions of the X-Bob (top) and LET (bottom) single unit.

Table 1: Original dimensions before FEA optimisation.

Mechanism	Dimension (mm)						
	L	h	d	t	w	z	Fillet
X-Bob	-	21.2	2.5	1	50	10	-
LET	5	21.2	2.5	1	50	10	1

Next, 5 shape iterations were developed from the original LET mechanism, using the dimensions from Table 1. The material stress and force output of the shapes were compared using the same prescribed displacement and material in FEA as above. The shape with the best stress distribution and highest SSF to force ratio was chosen.

Iteration Set 1 was conducted by optimising the dimensions of the chosen mechanism shape. Using the same FEA parameters as above, an iterative approach was conducted in which each key dimension was altered within a defined range (Table 2).

Dimensions were optimised sequentially while holding the others constant, in the order listed from top to bottom in Table 2. The most suitable value was chosen based on a high SSF to force ratio observed from the trends between dimension size and both stress and force, separately. The optimised value obtained for each dimension was used to update the set of dimensions prior to optimising the next.

Table 2: Range of values for key dimension optimisation.

Dimension	Minimum Value (mm)	Maximum Value (mm)
L	3	12
h	21	37
d	1.5	4
t	0.5	2
w	40	65
z	6	30
Fillet	0	3

After obtaining the final set of optimised values, Iteration Set 2 was conducted to account for effects of interdependencies between dimensions. Simulations were performed on the full mechanism design, comprised of 4 units in series. A prescribed displacement of 112 mm was applied, using the material properties of nylon-6-PLA sheets (as per the ASTM D638 standard). The stiffness and yield strength values were 3450 MPa and 75 MPa, respectively. Nylon-6-PLA was selected due to accessibility to fabricate the final design and its high stiffness and strength values, ideal for use in compliant mechanisms.

The geometry was optimised to reach the desired force output while minimising the material stress. Two mechanisms are to be integrated in the exoskeleton proof of concept, thus, the force requirement for one mechanism is 58.92 N, half of the total target force.

2.3 Experimental Testing

To evaluate the actual performance of the compliant mechanism, the design was manufactured from nylon-6-PLA sheets using CNC machining. A compression test was performed on the final prototype. The compression test setup can be seen in Figure 4.

Figure 4: Compression test setup.

The compression test speed was 250 mm/min, with a hold time of 30 seconds at the maximum machine extension. The limit for the test was set at 108mm. Force vs extension graphs were obtained from the compression tests, displaying the trend between force output and displacement of the mechanism.

3 Results and Discussion

The following sections present the FEA optimisation results, related experimental performance of the machined compliant mechanism and the final proof of concept.

3.1 Compliant Mechanism FEA

Shape Optimisation

A comparison between the X-Bob and LET mechanism demonstrated that the LET design had greater potential for integration into the Compli-Knee. The SSF of the X-Bob and LET mechanism was 0.3 and 1.75, respectively. Furthermore, the stress distribution maps (Figure 5) suggest the LET mechanism provides a more uniform stress distribution across the material. Although the force output of the X-Bob (65 N) was much higher than that of the LET mechanism (6.01 N), the significantly low SSF poses challenges for further optimisation. Improving the SSF would likely require reducing dimensions, causing the members to become too thin to be structurally viable.

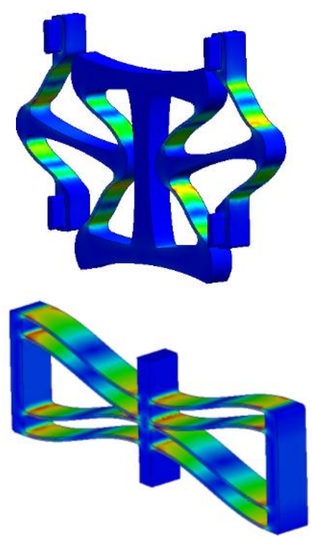

Figure 5: FEA stress map of the X-Bob (top) and LET (bottom) mechanism.

Despite the stress being distributed well across the LET mechanism, there were still indications of concentrated stress at the ends of the horizontal members. To address this localised stress, several shape iterations were explored, shown in Figure 6 along with the resulting stress maps. Only the left-hand side is illustrated due to the symmetrical nature of the design.

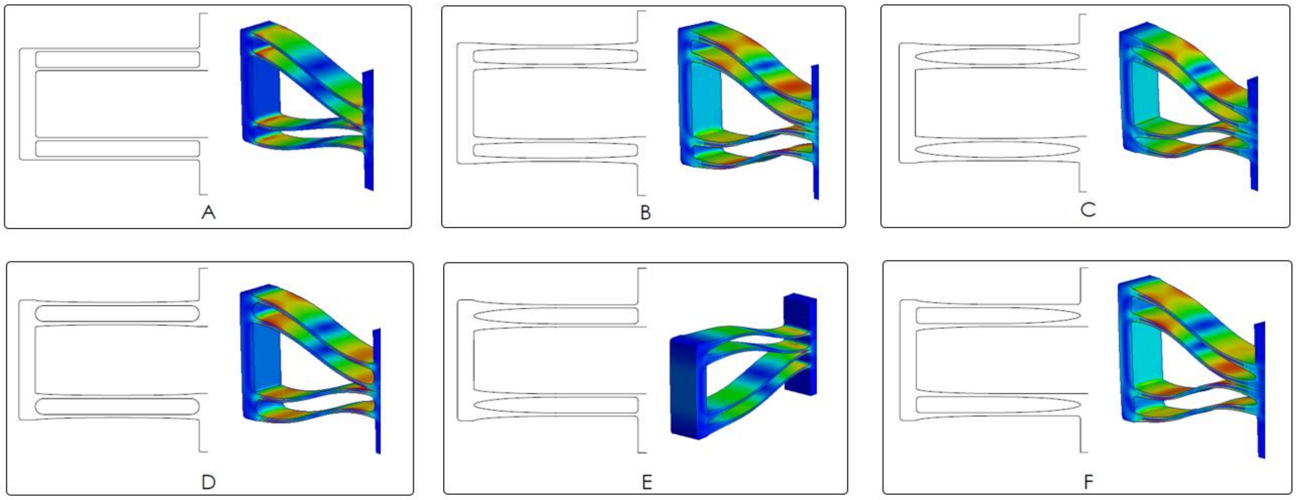

Figure 6: Left side of LET shape iterations: shape geometry (left) and FEA stress map (right). A: Original rectangle. B: External and internal partial ellipse. C: External partial ellipse with internal ellipse. D: External partial ellipse with internal slot. E: External partial ellipse with internal rectangle and ellipse combination (outward). F: External partial ellipse with internal rectangle and ellipse combination (inward).

The stress distribution across the horizontal members was improved for all cases, except Figure 6E where the stress remained concentrated on one end. The SSF for each shape was compared to the force output (Figure 7). Although Shape A and D had the highest SSF, their low force outputs limit their potential for integration in the Compli-Knee. In contrast, Shape C exhibited the highest force output, however, the SSF was low in comparison to most of the other shape iterations. Shape B was chosen for further optimisation due to the relatively high SSF and force results.

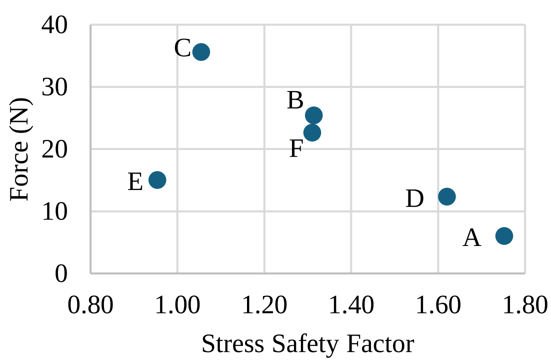

Figure 7: Comparison of force and stress safety factor for the LET shape iterations.

Dimension Optimisation

Sequential optimisation of the key dimensions (Iteration Set 1) demonstrated the extent to which each parameter effects the stress and force output of the mechanism. Figure 8 displays the stress and force range from changing the key measurements. Dimension L and h have minimal effect on the FEA results. These values were designed based on the smallest allowable size based on the required displacement and the chosen fillet size. Minimising L and h will ensure the design remains compact in size and lightweight for integration in the Compli-Knee.

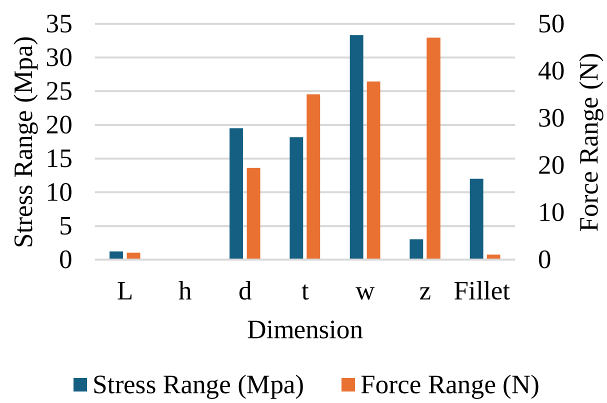

Figure 8: Effect of altering key dimensions on FEA stress and force output.

Dimensions d, t, and w had a significant effect on both FEA outputs, therefore, they were optimised using the trends shown in Figure 9. Additionally, z had a large influence on force output while having minimal effect on stress. Thus, optimisation of z was completed near the end of the iterative process to increase the force to the target value. The fillet had minimal effect on force output, however the stress showed a larger response in comparison. Analysing the trend of the fillet in Figure 9, it is apparent the fillet radius should be larger than 0.6mm to minimise the material stress.

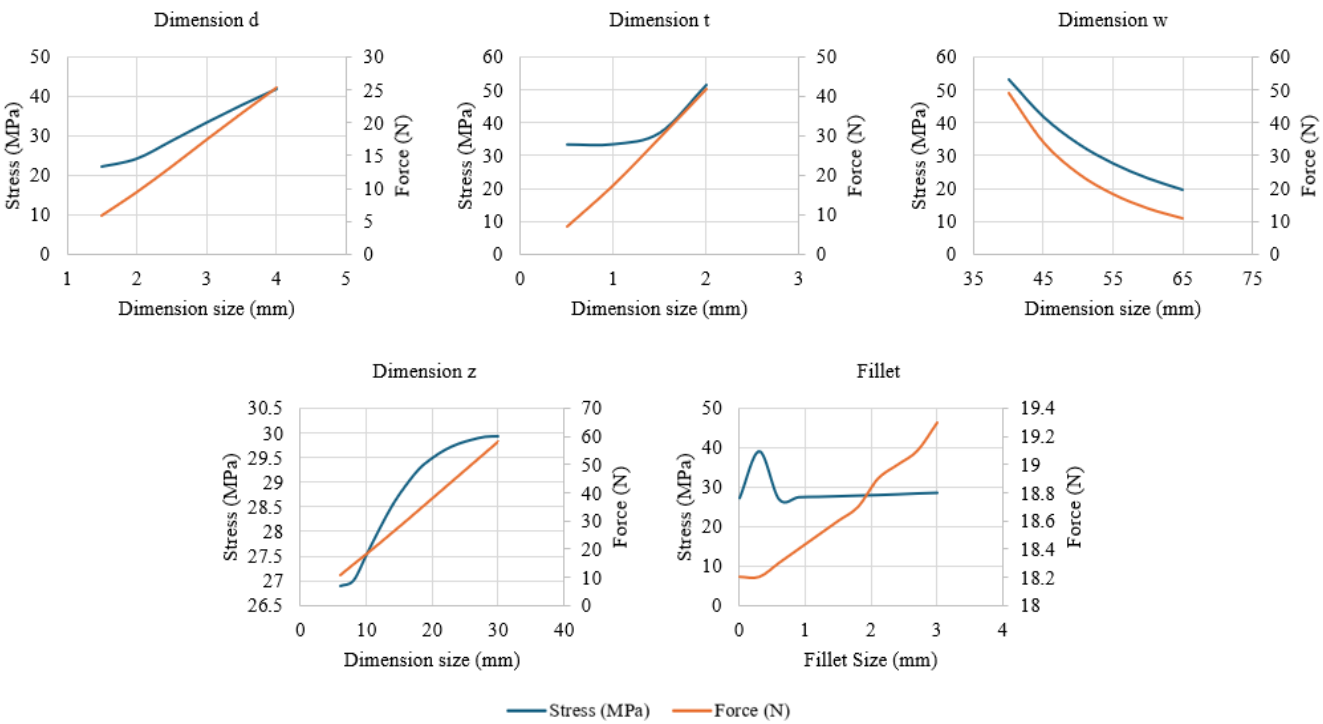

Figure 9: Trend between dimension size and the FEA stress and force output.

Further optimisation (Iteration Set 2) using nylon-6-PLA allowed for a larger displacement with a reduced number of units. This was achieved due to both further dimension adjustments and improved material properties. The SSF and force output achieved were also higher. The final dimensions and FEA performance of both iteration sets are presented in Table 3. Provided the final mechanism would be CNC machined, dimension t was increased to improve manufacturing accuracy. The fillet was increased to accommodate the minimum tool radius of the milling bit.

The final FEA results demonstrated that the LET mechanism achieved a SSF above the original baseline of 1.5 and can output 100% of the desired force. This corresponds to the ability of the mechanism to alleviate all of the knee moment for a 43.46 kg person during blueberry harvesting. Additionally, the stress was distributed well across the entire mechanism, as illustrated in Figure 10.

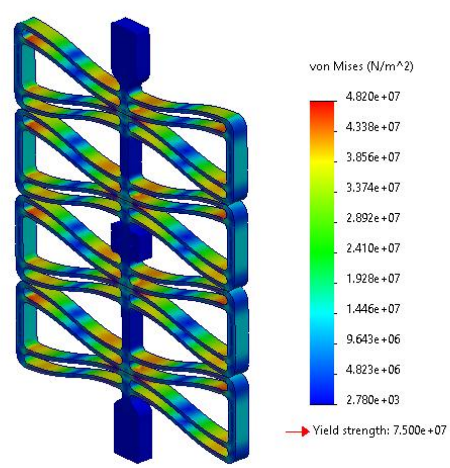

Figure 10: FEA stress map of the final LET mechanism.

Table 3: Optimised dimensions after each set of iterations.

Iteration Set	Dimension (mm)							No. of Units	Total Displacement (mm)	SSF	Force Output Relative to Desired Output
	L	t	d	w	h	z	Fillet				
Set 1	6	1.3	3	55	21.22	10	1.2	5	106.1	1.26	85.2 %
Set 2	6.6	2.1	3.042	82	28	9.7	2.8	4	112	1.56	100 %

3.2 Experimental Performance

Although FEA achieved a total displacement of 112 mm, the compression test only reached approximately 108 mm of displacement. Maximum compression occurs when dimension h is fully compressed for all units. Measuring the final fabricated mechanism showed that the h dimensions were on average 0.3 mm smaller than the SolidWorks model, equating to a total of 1.2 mm difference across the whole mechanism.

Additionally, in the vertical standing position, the total length of the fabricated mechanism was approximately 3.25 mm shorter than the SolidWorks model. It can be assumed that the weight of the mechanism caused premature compression of the system.

A linear relationship exists between the force output and deflection of the LET mechanism. Figure 11 relates the results to the percentage of knee joint moment alleviated and the knee flexion angle during deep squatting for a 43.46 kg user. Consideration was made to account for some forces acting axially along the thigh before reaching full flexion at 160°.

For the specified design requirements, the fabricated exoskeleton could alleviate 67% of a user's knee joint moment, suggesting a 33% deviation from the FEA simulation. This error can be attributed to the material properties used in the SolidWorks FEA simulation.

To obtain the material properties, the nylon-6-PLA sheets were tested shortly after being purchased. Although the dog-bone samples were placed in a humid chamber before testing to replicate the effects of moisture exposure, the diffusion coefficient of the material may impact how effective this method is. Having been subjected to constant moisture exposure for several months since testing, the stiffness of the sheets could have degraded, a common trend found in moisture exposed nylon [26].

Using an iterative approach, the stiffness of the nylon-6-PLA was altered in FEA to meet the maximum force output from the compression test (39.63 N). Reducing the material stiffness to 2400 MPa achieved a maximum force output with only 0.32% error to the compression test.

Using this revised value, FEA simulation for 7 different prescribed displacements was performed to imitate the compression test. Results show that the updated FEA aligns closely to the compression test results (Figure 11). This supports claims that degradation of the nylon-6-PLA material properties has caused the discrepancies between the FEA and experimental results.

Further work should look to test dog-bone samples of the nylon-6-PLA sheets used to confirm the cause. To account for the effects of moisture exposure, geometry optimisation should be performed using the material properties in wet conditions, such as a stiffness of 1700 MPa and yield strength of 45 MPa [27]. Furthermore, upon fabrication, the parts should be placed in water for a sufficient amount of time to reach full saturation.

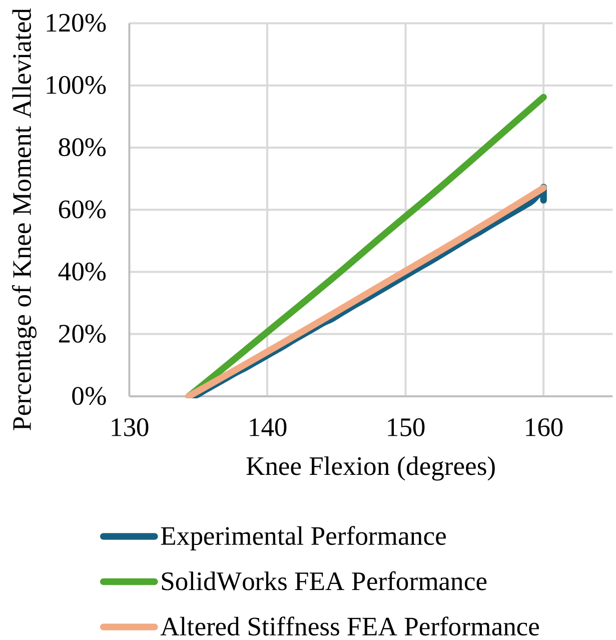

Figure 11: Knee joint moment alleviated for a 43.46 kg user vs knee flexion for the experimental and SolidWorks FEA performance.

Figure 11 shows that the experimental force decreased over time as the mechanism was held at maximum compression. Analysing the relationship between force and time for this period (Figure 12) indicated there is a non-linear decrease. A total reduction of 2.47 N occurred over 30 seconds. This reduction in force is likely due to elastic relaxation of the nylon-6-PLA. When removing the LET mechanism from the machine, the shape remained deformed by approximately 4 mm. However, the mechanism recovered to its original length when stretched by hand, suggesting no plastic deformation exists.

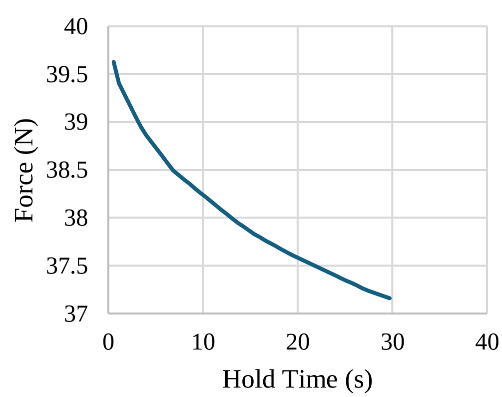

Figure 12: Change in mechanism force output when held at maximum compression.

Finally, the performance of the LET mechanism integrated in the Compli-Knee can be scaled to user mass. The percentage of knee moment alleviated across a range of user masses is shown in Figure 13. It is apparent that as user mass increases, the effect of mechanism decreases. This relationship begins to plateau for heavier individuals. The maximum value included is 130.14 kg based on the anthropometric data.

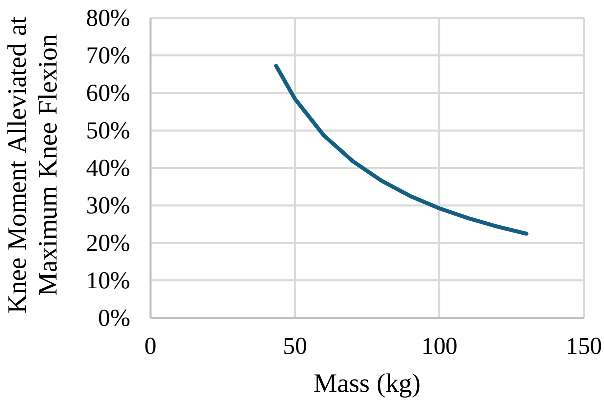

Figure 13: Knee moment alleviated based on user mass.

3.3 Integration of Compliant Mechanism in an Exoskeleton

Currently, no exoskeletons exist in literature for blueberry harvesting using compliant mechanisms. As a proof of concept, the LET mechanism was integrated into the Compli-Knee system, illustrated in Figure 14.

Figure 14: Exoskeleton system: Compli-Knee assembly (left) and engaged proof of concept on left leg (right).

Two mechanisms are included per leg, with one mechanism located on either side to provide a uniform force and eliminate undesired torque on the knee joint. Ongoing and future work looks to develop and evaluate a functioning prototype of the Compli-Knee.

4 Conclusion

This study successfully optimised a linear compliant mechanism for integration into a passive knee exoskeleton, designed to reduce knee moment for blueberry harvesters. FEA performance of the LET mechanism achieved 100% alleviation of knee moment for a 43.46 kg user. Compression testing concluded that the fabricated prototype achieved 67% alleviation. This discrepancy is attributed to the degradation of nylon-6-PLA material properties due to moisture exposure.

The Compli-Knee proof of concept demonstrates strong potential for integrating the LET mechanism. Future work will focus on optimising the compliant mechanism for heavier users, evaluating more durable materials for orchard conditions, and conducting field testing of the full prototype under real harvesting tasks.

Acknowledgements

This work was supported by the Ministry of Business, Innovation and Employment (MBIE), New Zealand, under grant UOWX2203. The authors gratefully acknowledge the technical staff at the School of Engineering, University of Waikato, for their valuable assistance and especially thank Brett Nichol for his help with experimental testing and setup. Additional thanks are due to peers and colleagues whose input and discussions informed this research.

References

[1] B. Farneti *et al.*, "Exploring Blueberry Aroma Complexity by Chromatographic and Direct-Injection Spectrometric Techniques," *Front. Plant Sci.*, vol. 8, p. 617, 2017, doi: 10.3389/fpls.2017.00617.

[2] Horticulture New Zealand, "About the horticulture industry in New Zealand," Horticulture New Zealand. Accessed: Sept. 18, 2025. [Online]. Available: https://www.hortnz.co.nz/about-us

[3] S. Murray, "Blueberry boom: Market set to expand as confidence grows," NZ Herald. Accessed: Sept. 18, 2025. [Online]. Available: https://www.nzherald.co.nz/the-country/news/blueberry-boom-market-set-to-expand-as-confidence-grows/MPIEKPC6YZBZ3JAOE7ODFJSZNY/

[4] E. Kim, A. Freivalds, F. Takeda, and C. Li, "Ergonomic Evaluation of Current Advancements in Blueberry Harvesting," *Agronomy*, vol. 8, no. 11, Art. no. 11, Nov. 2018, doi: 10.3390/agronomy8110266.

[5] O. Thamsuwan, S. Milosavljevic, D. Srinivasan, and C. Trask, "Potential exoskeleton uses for reducing low back muscular activity during farm tasks," *Am. J. Ind. Med.*, vol. 63, no. 11, pp. 1017–

1028, 2020, doi: 10.1002/ajim.23180.
[6] V. Wilkinson and T. Morris, “Opportunities in the New Zealand Blueberry Industry,” July 2020.
[7] Wageningen Food & Biobased Research, “Harvest practices for blueberries,” freshknowledge.eu. Accessed: Sept. 18, 2025. [Online]. Available: https://www.freshknowledge.eu/en/increase-your-knowledge/crops/blueberry/harvest-practices-for-blueberries.htm
[8] R. K. Gallardo *et al.*, “Blueberry Producers’ Attitudes toward Harvest Mechanization for Fresh Market,” Feb. 2018, doi: 10.21273/HORTTECH03872-17.
[9] A.-D. Danko and M. Straka, “Exoskeletons - Robotic Suits Improving Work in Logistics,” *Acta Logist.*, vol. 9, no. 4, pp. 405–410, Dec. 2022, doi: 10.22306/al.v9i4.332.
[10] L. L. Howell, S. P. Magleby, and B. M. Olsen, *Handbook of Compliant Mechanisms*. Newark, UNITED KINGDOM: John Wiley & Sons, Incorporated, 2013. Accessed: Mar. 13, 2025. [Online]. Available: http://ebookcentral.proquest.com/lib/waikato/detail.action?docID=1119456
[11] Y. Niu, Z. Song, and J. Dai, “Kinematic analysis and optimization of a planar parallel compliant mechanism for self-alignment knee exoskeleton,” *Mech. Sci.*, vol. 9, no. 2, pp. 405–416, Nov. 2018, doi: 10.5194/ms-9-405-2018.
[12] H. K. Kwa, J. H. Noorden, M. Missel, T. Craig, J. E. Pratt, and P. D. Neuhaus, “Development of the IHMC Mobility Assist Exoskeleton,” in *2009 IEEE International Conference on Robotics and Automation*, May 2009, pp. 2556–2562. doi: 10.1109/ROBOT.2009.5152394.
[13] J. E. Pratt, B. T. Krupp, C. J. Morse, and S. H. Collins, “The RoboKnee: an exoskeleton for enhancing strength and endurance during walking,” in *IEEE International Conference on Robotics and Automation, 2004. Proceedings. ICRA ’04. 2004*, Apr. 2004, pp. 2430-2435 Vol.3. doi: 10.1109/ROBOT.2004.1307425.
[14] J. Song, A. Zhu, Y. Tu, X. Zhang, and G. Cao, “Novel Design and Control of a Crank-Slider Series Elastic Actuated Knee Exoskeleton for Compliant Human–Robot Interaction,” *IEEEASME Trans. Mechatron.*, vol. 28, no. 1, pp. 531–542, Feb. 2023, doi: 10.1109/TMECH.2022.3204921.
[15] S. Jin, R. McCulloch, and G. A. Mirka, “Biomechanical evaluation of postures assumed when harvesting from bush crops,” *Int. J. Ind. Ergon.*, vol. 39, no. 2, pp. 347–352, Mar. 2009, doi: 10.1016/j.ergon.2008.07.005.
[16] A. Forner-Cordero *et al.*, “Kinematics and Dynamics of Wearable Robots,” in *Wearable Robots*, John Wiley & Sons, Ltd, 2008, pp. 47–85. doi: 10.1002/9780470987667.ch3.
[17] U. Glitsch, K. Heinrich, and R. P. Ellegast, “Estimation of Tibiofemoral and Patellofemoral Joint Forces during Squatting and Kneeling,” *Appl. Sci.*, vol. 12, no. 1, Art. no. 1, Jan. 2022, doi: 10.3390/app12010255.
[18] T. Nagura, C. O. Dyrby, E. J. Alexander, and T. P. Andriacchi, “Mechanical loads at the knee joint during deep flexion,” *J. Orthop. Res.*, vol. 20, no. 4, pp. 881–886, 2002, doi: 10.1016/S0736-0266(01)00178-4.
[19] Y. Zhou, X. Wang, X. Tang, X. Ji, and Z. Gao, “Design and analysis of a passive knee assisted exoskeleton,” *Adv. Mech. Eng.*, vol. 15, no. 11, p. 16878132231202578, 2023, doi: 10.1177/16878132231202578.
[20] M. C. Gonzalez, A. Mehrnezhad, N. Razaviarab, T. G. Barbosa-Silva, and S. B. Heymsfield, “Calf circumference: cutoff values from the NHANES 1999–2006,” *Am. J. Clin. Nutr.*, vol. 113, no. 6, pp. 1679–1687, June 2021, doi: 10.1093/ajcn/nqab029.
[21] G. Karimi and O. Jahanian, “(PDF) Genetic Algorithm Application in Swing Phase Optimization of AK Prosthesis with Passive Dynamics and Biomechanics Considerations,” in *ResearchGate*, 2012. doi: 10.5772/38211.
[22] I. Kiefer, B. Leitner, R. Bauer, and A. Rieder, “Body weight: The male and female perception,” *Soz.- Präventivmedizin*, vol. 45, no. 6, pp. 274–278, Nov. 2000, doi: 10.1007/BF01591690.
[23] D. Šentija, M. Rakovac, and V. Babić, “Anthropometric characteristics and gait transition speed in human locomotion,” *Hum. Mov. Sci.*, vol. 31, no. 3, pp. 672–682, June 2012, doi: 10.1016/j.humov.2011.06.006.
[24] X. Zhou, G. Liu, B. Han, L. Wu, and H. Li, “Design of a Human Lower Limbs Exoskeleton for Biomechanical Energy Harvesting and Assist Walking,” *Energy Technol.*, vol. 9, no. 1, p. 2000726, 2021, doi: 10.1002/ente.202000726.
[25] J. Zelle, M. Barink, M. De Waal Malefijt, and N. Verdonschot, “Thigh–calf contact: Does it affect the loading of the knee in the high-flexion range?,” *J. Biomech.*, vol. 42, no. 5, pp. 587–593, Mar. 2009, doi: 10.1016/j.jbiomech.2008.12.015.
[26] J.-C. Huang, T.-H. Wu, and C.-L. Wu, “Effects of Moisture on Mechanical Properties of Glass-Filled Nylon-6,6,” *ResearchGate*, 1995, doi: 10.1515/SECM.1995.4.3.199.
[27] “Comparative Physical Properties: LEP Engineering Plastics.” LEP: Engineering Plastics. Accessed: Sept. 25, 2025. [Online]. Available: https://lep.co.nz/wp-content/uploads/2016/02/Engineering-Plastics-Physical-Properties.pdf